RSC Advances

ROYAL SOCIETY OF CHEMISTRY

www.rsc.org/advances

Journal Name

COMMUNICATION

A Dithienodisilacyclohexadienes (DTDS)-Based Conjugated Model Semiconductor: Understanding Unique Features and Monitoring Structural Transition

Received 00th January 20xx,
Accepted 00th January 20xx

DOI: 10.1039/x0xx00000x

www.rsc.org/

Tao Cheng, Shanshan Chen, Kyu Cheol Lee, Sang Myeon Lee and Changduk Yang*

To enable a superior σ*–π* conjugation, we present a dithienodisilacyclohexadienes(DTS) analogue of DTS(FBTTh$_2$)$_2$–namely, DTDS(FBTTh$_2$)$_2$–by replacing dithienosilole(DTS) with a dithienodisilacyclohexadienes(DTDS) ring in the main backbone, where DTDS possesses a double silicon-bridged bithiophene (Si–Si). With this replacement, a blue shift of the absorption and high-lying LUMO are observed. Disclosed herein is a structural change of DTDS(FBTTh$_2$)$_2$ (DTDS to ox-DTDS skeleton as the corresponding oxidation structure) occurring in ambient condition, which is monitored by real-time ^{1}H NMR and UV absorption methods. This work not only provides a full understanding of the nature of DTDS, but also uses unique DTDS chemistry as a new toolbox to develop systems as novel functionality materials.

Since the discovery that siloles composed of five-membered silacyclics possess σ*–π* conjugation between π-symmetrical σ* orbital of two exocyclic σ-bonds on silicon and π* orbital of the butadiene moiety,[1] many research groups have been investigating the silole-containing conjugated materials to benefit from their unique optical and semiconducting properties, paving the way to the emergence of the fields of plastic electronics and photonics.[2] A particularly interesting framework associated with the silole is a tricyclic dithienosilole (DTS) with a intramolecular organosilanylene bridge at the *β, β′*-position of a bithiophene unit (**Fig.1**).[3] Owing to its high co-planarity and low-lying LUMO energy level arising from the σ*–π* conjugation, DTS has been extensively studied as a promising electron-rich block of push-pull fashion along the backbone. Among this class of molecules, 7,7′-(4,4-bis(2-ethylhexyl)-4*H*-silolo[3,2-*b*:4,5-*b′*]dithiophene-2,6-diyl)bis(6-fluoro-4-(5′-hexyl-[2,2′-bithiophen]-5-yl)benzo[*c*][1,2,5]thiadiazole), DTS(FBTTh$_2$)$_2$ (**Fig. 1**) in particular has been subject to increasing interest in the photovoltaic community, but significant progress has also been made in understanding its intrinsic properties.[4]

Considering the fact that the insertion of two silicon atoms in the ring (disilanylene (Si–Si)-bridged bithiophene) can further enhance the σ*–π* conjugation, the DTDS (see **Fig. 1**) was first synthesized and characterized by Ohshita and co-workers in 1998,[3b] and introduced as an emerging building block of conjugated polymers and demonstrated the excellent photovoltaic performance recently.[5] These intriguing results inspire us to replace DTS with DTDS in the DTS(FBTTh$_2$)$_2$ as an extension of the study concerning the chemistry of the siloles, aiming not only to clearly understand the nature of the DTDS skeleton but also to uncover the potential utility of the DTDS-containing conjugated systems as novel functionality materials.

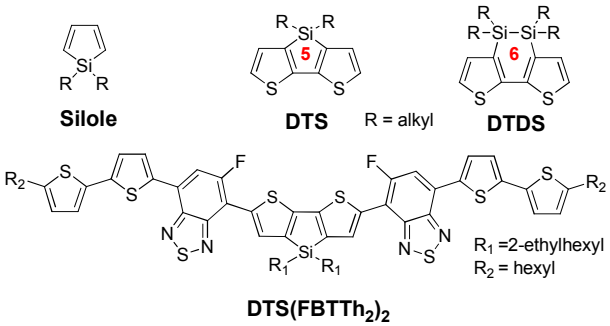

Fig.1. Representative molecular structures based on silole unit

In this study, we report the synthesis, structure, and properties of DTDS(FBTTh$_2$)$_2$ in detail. Notably, we found that the Si–Si unit in DTDS was converted to siloxane (Si–O–Si) bond, when handled without special care. To obtain definitive evidence to the Si–O–Si conformation, we also synthesized the corresponding oxadithienodisilacycloheptadiene (ox-DTDS)-based oxidation derivatives and carefully characterized them in a comparative manner. The synthetic routes to the key bis-stannylated DTDS monomer **3** and the target product DTDS(FBTTh$_2$)$_2$ are depicted in **Scheme 1**, and the detailed synthesis procedure is described in the Supplementary Information.

Department of Energy Engineering, School of Energy and Chemical Engineering. Ulsan National Institute of Science and Technology (UNIST) Ulsan 689-798, South Korea. E-mail: yang@unsit.ac.kr
Electronic Supplementary Information (ESI) available:See DOI: 10.1039/x0xx00000x

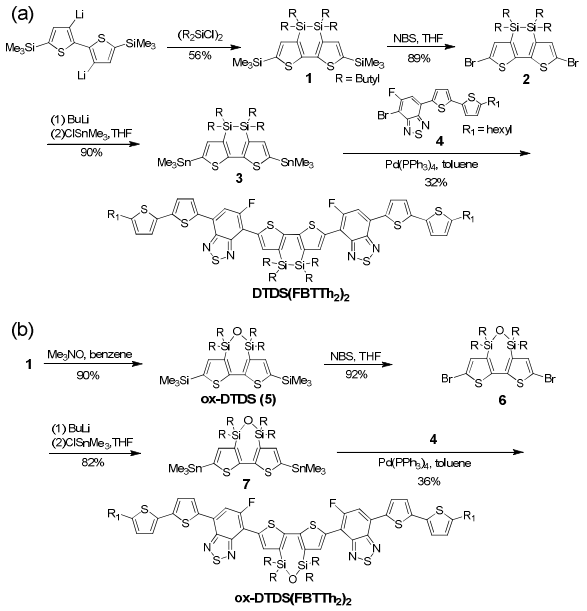

Scheme 1. Synthetic routes to DTDS(FBTTh$_2$)$_2$ (a) and ox-DTDS(FBTTh$_2$)$_2$(b).

As reported, bis-silylated DTDS **1** was readily synthesized by a coupling reaction between 1,2-dichlorotetrabutyldisilane and 3,3′-dilithio-5,5′-bis(trimethylsilyl)-2,2′-bithiophene in a 56% yield, followed by treatment of *N*-bromosuccinimide (NBS), which afforded dibromide compound **2**. After workup and purification of the bromination, although the identity and purity of **2** seemed to be supported by the completely assigned peaks of the ^{1}H NMR spectrum, some of the undefined small resonances were observed in the aromatic region of the ^{13}C NMR (see **Fig. 2**).This leads us to believe that the stability of the Si–Si bond in DTDS is insufficient under oxidative conditions, presumably forming the Si–O–Si bond to a certain extent. As following a reported method,[6] for substantiating this hypothesis, the compound **1** was treated with excess trimethylamine *N*-oxide, an oxidizing agent, which produced the corresponding ox-DTDS compound **5**,[6] which was subsequently converted into the dibromide **6** via the NBS with overall two-step yield of 83%. Due to the very similar chemical shifts in the aromatic proton peaks of **2** (δ = 6.946 ppm) and **6** (δ = 6.948 ppm), we were not able to pinpoint and identify the structures by using ^{1}H NMR data. However, in a comparative inspection of their ^{13}C NMR spectra, we confirm that all additional peaks mentioned above for **2** are correlated with the carbon resonances, belonging to **6**. Note that with solid evidence for the traces of **6** in the synthesized **2**, attempts to further purify **2** for high quality were unsuccessful. Thereby, without full elimination of **6**, the required bis-stannylated DTDS monomer **3** was obtained from a typical lithiation/stannylation of **2** at low temperature, which was then used in the last step of the synthetic sequence. The target DTDS(FBTTh$_2$)$_2$was synthesized via a Stille cross-coupling reaction between the molecular "core" of bis-stannylated DTDS and the previously reported mono-brominated molecular "wing" of **4**. As above-mentioned, despite the myriad difficulties in separating pure DTDS monomers, the pure DTDS(FBTTh$_2$)$_2$ was obtained by a combination of column chromatography, extraction mixture solution (Hexane: MeOH, 3:1% v/v), and recrystallization from acetone. The purification steps were repeated once to give absolute DTDS(FBTTh$_2$)$_2$as a metallic deep purple solid, the purity of which was determined by NMR spectroscopy and mass spectrometry (see **Fig. S1**).

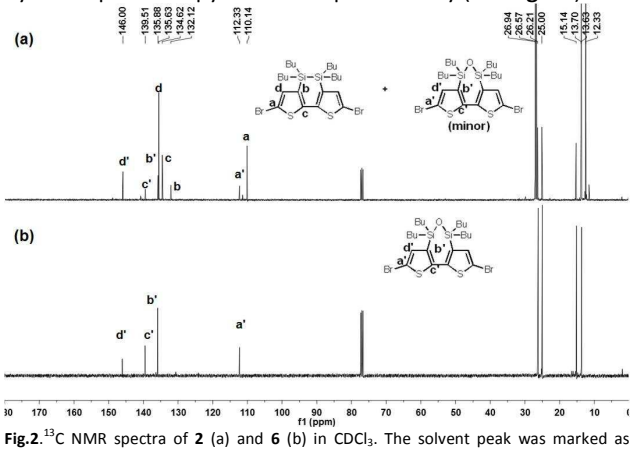

Fig.2.^{13}C NMR spectra of **2** (a) and **6** (b) in $CDCl_3$. The solvent peak was marked as asterisk.

Surprisingly, the deep purple of DTDS(FBTTh$_2$)$_2$ in chloroform solution placed in the hood was gradually changed to a deep red one in the course of time, indicative of a dramatic structural change under ambient conditions, which is most likely attributed to the ox-DTDS formation. To better understand the inherent properties of this new class and with the aim of establishing design principles toward the DTDS-containing structural analogues as multiple potential utilities, not only did we synthesize ox-DTDS(FBTTh$_2$)$_2$ from the same procedure above using ox-DTDS core instead of DTDS (see SI for full experimental details), but we also carried out the real-time NMR experiments of DTDS(FBTTh$_2$)$_2$ to monitor the sequential structure dynamics.

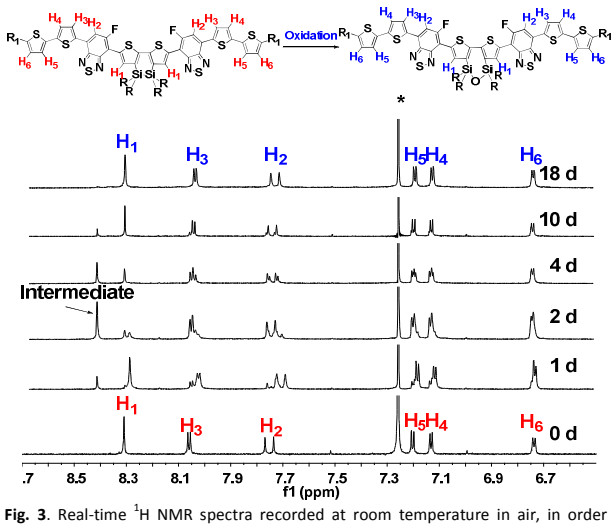

Fig. 3. Real-time ^{1}H NMR spectra recorded at room temperature in air, in order to monitor the structural transitioning from DTDS(FBTTh$_2$)$_2$ to ox-DTDS(FBTTh$_2$)$_2$. The solvent peak was marked as asterisk.

The aromatic regions of the ^{1}H NMR spectra of DTDS(FBTTh$_2$)$_2$ in $CDCl_3$ are shown in **Fig. 3**. For the freshly prepared DTDS(FBTTh$_2$)$_2$, six distinct aromatic proton resonances were clearly observed. As a function of time, the intensity of the thiophene resonance (H_1) of DTDS unit (8.31 ppm) decreased, while a new sharp resonance appeared at 8.43 ppm. The shifting of the signals (8.31 to 8.43 ppm) was almost completed after 2 days, indicating the formation of other species as intermediates.

Very surprisingly, the furthest downfield singlet at 8.43 ppm underwent a subsequent decrease in the intensity, together with the emergence of another new resonance at 8.33 ppm in the extended periods (~ 4 days). The conversion process was complete after 18 days, finally enabling access to well-defined resonances, which was authenticated as having molecular structure identical to that of ox-DTDS(FBTTh$_2$)$_2$ after thorough comparative analysis of NMR and mass data (see **Fig. S2** for mass spectroscopy depending on time).

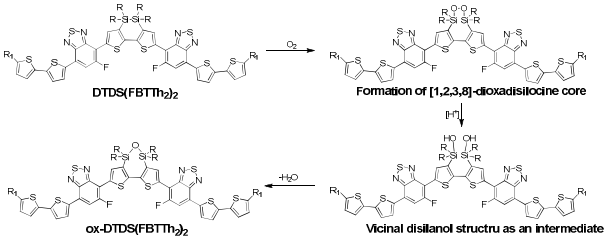

Scheme 2. A rational mechanism proposed to explain the structural transition in air.

Scheme 2 shows a plausible conversion mechanism for the formation of ox-DTDS(FBTTh$_2$)$_2$ in air. In the initial step, a molecular oxygen attached at Si–Si unit of DTDS to form the [1,2,3,8]-dioxadisilocine core. Upon opening and contact with moisture of the air in the extended periods of time, the Si–O–O–Si group in the dioxadisilocine group was hydrolyzed to give a vicinal disilanol intermediate because of its high reactivity. Finally, ox-DTDS(FBTTh$_2$)$_2$ could be thermodynamically obtained from the intra-dehydration process to generate a more stable Si–O–Si linkage.

Absorption spectra of DTDS(FBTTh$_2$)$_2$are shown in **Fig. 4a**. In chloroform, DTDS(FBTTh$_2$)$_2$shows intramolecular charge transfer absorption typical of chromophores with push-pull architecture. This exhibits low-energy transition with a maximum at 556 nm and a molar absorption coefficient of 8.75×10^4 M^{-1} cm^{-1}. The absorption maximum is red-shifted approximately 10 nm in thin films cast from chloroform. From the onset of the absorption (694 nm), the solid-state optical bandgap was estimated to be 1.78 eV, which is quite comparable to that of the archetypical polymer P3HT, often referred to as the "fruit fly" of organic semiconductors.[7] This is a slightly wider bandgap compared to that of DTS(FBTTh$_2$)$_2$, whose solid-state absorption onset at 747 nm suggests a band gap of 1.66 eV.[8] Note that the replacement of DTDS with ox-DTDS results in blue-shifted absorption for DTDS(FBTTh$_2$)$_2$ in solution as well as in the solid state versus ox-DTDS(FBTTh$_2$)$_2$, reflecting the lower degree of co-planarity induced by Si–O–Si groups (see **Fig. S3**).

By utilizing solution cyclic voltammetry (CV), the HOMO and LUMO energy levels of DTDS(FBTTh$_2$)$_2$ were calculated to be -5.17 and -3.49 eV, respectively, using the ferrocene-ferrocenium (Fc/Fc^+) redox couple (4.88 eV below the vacuum level)(**Fig. 4b**). Based on a comparison of the frontier molecular orbitals of DTDS(FBTTh$_2$)$_2$ with respect to DTS(FBTTh$_2$)$_2$(HOMO/LUMO = -5.20/-3.74 eV),[8] it is found that the substitution of DTDS for the central DTS gives rise to a large change to a 0.25 eV higher-lying LUMO level, while maintaining a nearly identical HOMO level. It is worth pointing out that the increase in both the bandgap and energy levels observed for DTDS(FBTTh$_2$)$_2$ differs from the trends in the DTDS-related polymer system,[5] where the incorporation of DTDS in place of DTS into polymer backbone leads to a decrease in both HOMO and LUMO levels with a similar bandgap, when compared to the DTS-containing analogue. One possibility is that the more disordered backbone structure blurs subtle influences by stronger interaction between the σ*– and π*–orbitals derived from DTDS on optical and electrochemical transitions.

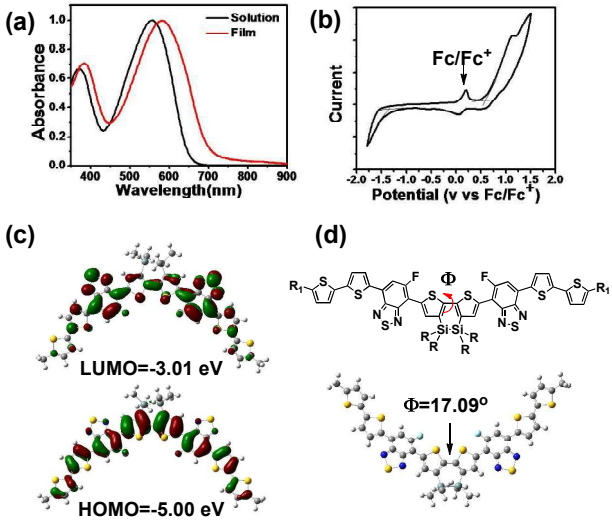

Fig. 4. Absorption spectra of DTDS(FBTTh$_2$)$_2$ in solution and films (a),cyclic voltammetry of DTDS(FBTTh$_2$)$_2$ film (b), and energy-minimized structure at the B3LYP/6-31G level (c and d).

Computational studies using density-functional theory (DFT, B3LYP/6-31G) approaches were carried out on DTDS(FBTTh$_2$)$_2$ with the alkyl chains replaced by methyl groups for simplicity. As shown in **Fig. 4c** and **d**, the HOMO is well-distributed along the conjugated chains, while the LUMO is mainly centralized on electron deficient FBT units as shaped by orbital lobes. We note that "U"-shaped structures are observed for both the optimized HOMO and LUMO is on surfaces, which are almost the same as those of DTS(FBTTh$_2$)$_2$.[9] Besides, it was confirmed that DTDS(FBTTh$_2$)$_2$involved a non-planar tricyclic DTDS system with a dihedral twist angle of 17.09° between the two thiophene rings. A detailed investigation on ox-DTDS(FBTTh$_2$)$_2$ such as UV, CV, and DFT can be found in Supplementary Information as relevant information for further understanding

the DTDS(FBTTh$_2$)$_2$ as a function of molecular structure and electronic state.

In summary, by taking into account the previously reported fascinating properties of DTS(FBTTh$_2$)$_2$ arising from the σ*-orbital of the silicon atom in DTS core, we have synthesized a DTDS-based analogue, DTDS(FBTTh$_2$)$_2$, in which DTDS involves a double silicon-bridged bithiophene (Si–Si). In this study, an intra-structural transitioning from Si–Si to Si–O–Si units in DTDS(FBTTh$_2$)$_2$ is not only confirmed by real-time ^{1}H NMR experiments, but the conversion mechanism is also formulated. Besides, we find that replacement of DTS with DTDS in π-conjugated systems leads to a selective fine-tuning of LUMO to a higher-lying level as well as a blue-shifted absorption. The upfront investment on this new platform of π-conjugated systems should open the door for research on DTDS-based distinct chemistry.

This work was supported by the National Research Foundation of Korea (NRF) grant funded by the Korea government (MSIP) (2015R1A2A1A10053397) and the 2015 Research Fund (1.150120.01) of UNIST (Ulsan National Institute of Science & Technology)

Notes and references

1. S. Yamaguchi and K. Tamao, *Bull. Chem. Soc. Jpn.*, 1996, **69**, 2327.
2. (a) K. Tamao, M. Uchida, T. Izumizawa, K. Furukawa and S. Yamaguchi, *J. Am. Chem. Soc.*, 1996, **118**, 11974; (b) K. Tamao, S. Yamaguchi, Y. Ito, Y. Matsuzaki, T. Yamabe, M. Fukushima and S. Mori, *Macromolecules*, 1995, **28**, 8668; (c) K. Tamao, S. Ohno and S. Yamaguchi, *Chem. Commun.*, 1996, 1873; (d) M. S. Liu, J. Luo and A. K. Y. Jen, *Chem. Mater.*, 2003, **15**, 3496; (e) J. Ohshita, D. Hamamoto, K. Kimura and A. Kunai, *J. Organomet. Chem.*, 2005, **690**, 3027.
3. (a) J. Ohshita, M. Nodono, T. Watanabe, Y. Ueno, A. Kunai, Y. Harima, K. Yamashita and M. Ishikawa, *J. Organomet. Chem.*, 1998, **553**, 487; (b) J. Ohshita, M. Nodono, H. Kai, T. Watanabe, A. Kunai, K. Komaguchi, M. Shiotani, A. Adachi, K. Okita, Y. Harima, K. Yamashita and M. Ishikawa, *Organometallics*, 1999, **18**, 1453.
4. (a) T. S. van der Poll, J. A. Love, T. Q. Nguyen and G. C. Bazan, *Adv. Mater.*, 2012, **24**, 3646; (b) V. Gupta, A. K. Kyaw, D. H. Wang, S. Chand, G. C. Bazan and A. J. Heeger, *Sci. Rep.*, 2013, **3**, 1965; (c) A. K. Kyaw, D. H. Wang, V. Gupta, J. Zhang, S. Chand, G. C. Bazan and A. J. Heeger, *Adv. Mater.*, 2013, **25**, 2397.
5. J. Ohshita, M. Nakashima, D. Tanaka, Y. Morihara, H. Fueno and K. Tanaka, *Polym. Chem.*, 2014, **5**, 346.
6. Y.-W. Kwak, I.-S. Lee, M.-K. Baek, U. Lee, H.-J. Choi, M. Ishikawa, A. Naka, J. Ohshita, K.-H. Lee and A. Kunai, *Organometallics*, 2006, **25**, 48.
7. (a) J. Hou, Z. Tan, Y. Yan, Y. He, C. Yang and Y. Li, *J. Am. Chem. Soc.*, 2006, **128**, 4911; (b) I. McCulloch, M. Heeney, C. Bailey, K. Genevicius, I. Macdonald, M. Shkunov, D. Sparrowe, S. Tierney, R. Wagner, W. Zhang, M. L. Chabinyc, R. J. Kline, M. D. McGehee and M. F. Toney, *Nat. Mater.*, 2006, **5**, 328.
8. M. Moon, B. Walker, J. Lee, S. Y. Park, H. Ahn, T. Kim, T. H. Lee, J. Heo, J. H. Seo, T. J. Shin, J. Y. Kim and C. Yang, *Adv. Energy Mater.*, 2015, DOI: 10.1002/aenm.201402044.
9. (a) L. F. Lai, J. A. Love, A. Sharenko, J. E. Coughlin, V. Gupta, S. Tretiak, T. Q. Nguyen, W. Y. Wong and G. C. Bazan, *J. Am. Chem. Soc.*, 2014, **136**, 5591; (b) X. Liu, Y. Sun, B. B. Hsu, A. Lorbach, L. Qi, A. J. Heeger and G. C. Bazan, *J. Am. Chem. Soc.*, 2014, **136**, 5697.